Publication III

Paukkunen, AK, Kurttio, AA, Leminen, MM, Sepponen, RE. A compact EEG recording device with integrated audio stimulation system. Review of Scientific Instruments, 81(6):064301, doi:10.1063/1.3436634, 2010.

© 2010 American Institute of Physics.
Reprinted with permission.

A compact electroencephalogram recording device with integrated audio stimulation system

Antti K. O. Paukkunen,[1,2] Anttu A. Kurttio,[1] Miika M. Leminen,[3,4] and Raimo E. Sepponen[1]
[1]*Department of Electronics, School of Science and Technology, Aalto University, Aalto 00076, Finland*
[2]*Graduate School of Electrical and Communications Engineering, School of Science and Technology, Aalto University, Aalto 00076, Finland*
[3]*Cognitive Brain Research Unit, Institute of Behavioral Sciences, Helsinki University, University of Helsinki, Helsinki 00014, Finland*
[4]*Finnish Centre of Excellence in Interdisciplinary Music Research, University of Helsinki, Helsinki 00014, Finland*

(Received 8 March 2010; accepted 1 May 2010; published online xx xx xxxx)

A compact ($96\times128\times32$ mm^3, 374 g), battery-powered, eight-channel electroencephalogram recording device with an integrated audio stimulation system and a wireless interface is presented. The recording device is capable of producing high-quality data, while the operating time is also reasonable for evoked potential studies. The effective measurement resolution is about 4 nV at 200 Hz sample rate, typical noise level is below 0.7 μV_{rms} at 0.16–70 Hz, and the estimated operating time is 1.5 h. An embedded audio decoder circuit reads and plays wave sound files stored on a memory card. The activities are controlled by an 8 bit main control unit which allows accurate timing of the stimuli. The interstimulus interval jitter measured is less than 1 ms. Wireless communication is made through bluetooth and the data recorded are transmitted to an external personal computer (PC) interface in real time. The PC interface is implemented with LABVIEW® and in addition to data acquisition it also allows online signal processing, data storage, and control of measurement activities such as contact impedance measurement, for example. The practical application of the device is demonstrated in mismatch negativity experiment with three test subjects. © *2010 American Institute of Physics.* [doi:10.1063/1.3436634]

I. INTRODUCTION

A typical instrument setup applied in auditory evoked potential (AEP) studies includes an electroencephalogram (EEG) amplifier, audio stimulation device, electrode cap, headphones, data acquisition system, and operator interface. Depending on the application, other stimulation devices (visual or tactile), for example, or response buttons for test subject interaction may be needed too. In order to be generally applicable, the structure of measurement systems is modular and they are implemented in pieces so that they can easily be modified. Thus, there are typically separate units for each function, which are connected in a way that also allows the integration of supplementary instrumentation.

This kind of a modular design gives flexibility in experiment design which is advantageous for research purposes. In routine investigations, however, the need for variability is typically small. Thus, the equipment can instead be optimized with respect to practical usability. In this study, a prototype of a compact eight-channel EEG recording device with integrated audio stimulation is presented. All the measurement-related electronics are integrated into one compact, battery-powered head box which is controlled from a personal computer (PC) interface through a bluetooth connection. The technical performance is first verified by measurements and its practical application demonstrated with three test subjects.

Compared to commercially available technology, the design presented here is simpler and setting up the experiments is therefore faster. This allows fast installation and an easy access to recording target activity. Eight channels give enough spatial resolution for credible studies[1,2] and less cabling means fewer interference paths through the wiring.[3] Fast preparation is particularly important in pediatric studies or if the test subject is restless, and an enhanced signal-to-noise ratio (SNR) improves the comparability of average responses.[4,5] Greater mobility is of practical significance, particularly in field applications.

II. MATERIAL AND METHODS

A. System description

The prototype consists of five main blocks (Fig. 1): the EEG recording hardware, contact impedance tester, audio stimulation system, data processing, and user interface. The first three are integrated into a wireless, battery-powered head box [Fig. 2(a)], at the heart of which is an 8-bit main control unit (MCU) (ATMEGA2560, Atmel Corp., USA). The MCU controls the stimulation and recording activities, and takes care of communication with the PC interface via bluetooth (WT12, Bluegiga Technologies Ltd., Finland).

The data processing and user interface [Fig. 2(b)] are in the PC interface, which is implemented using a graphical programming language (LABVIEW® 8.2, National Instruments, USA). Data processing means acquisition, online signal processing, and storage, and the user interface provides

 © 2010 American Institute of Physics

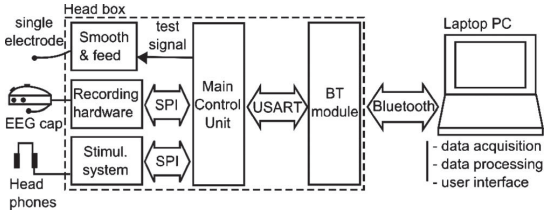

FIG. 1. The block diagram of the prototype system. The audio stimulation system, EEG recording hardware, and the contact tester are integrated into the head box. The user interface and the data processing system are in the PC interface. Communication between the devices takes place via bluetooth (BT).

tools for documentation, measurement control, and contact impedance testing. In addition, together, these also allow the accumulation of the average waveforms to be monitored online. Despite the complexity, the interface software is relatively light and it runs on a regular laptop PC (Intel® Pentium M, 1.73 GHz, 1 GB RAM, WINDOWS® XP professional).

B. EEG amplifier

The EEG is recorded from eight common ground-referenced channels using Ag/AgCl electrodes (Fig. 3). The common ground is formed at the first amplifier stage through

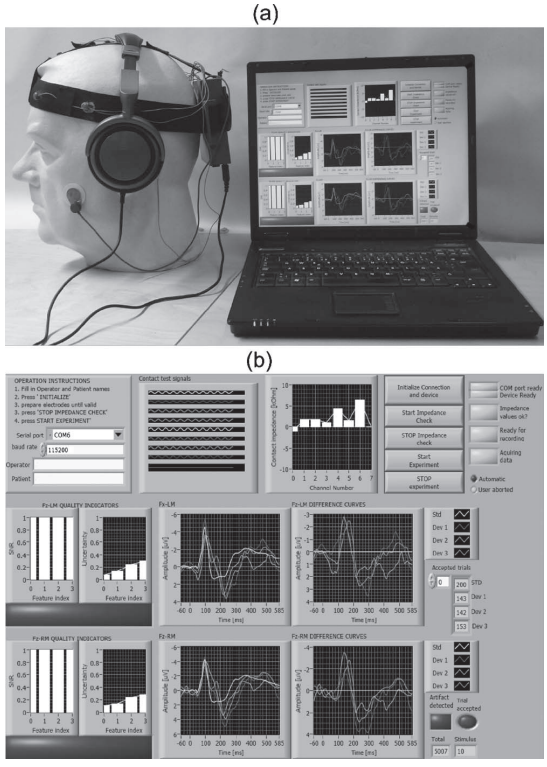

FIG. 2. The prototype implemented and the user interface. (a) The head box is battery powered and wireless and it can be attached to the electrode cap during the experiment. The dimensions are small ($96\times128\times32$ mm^3; weight: 374 g). (b) The PC interface provides basic operator functions and allows the average waveforms to be processed and monitored online.

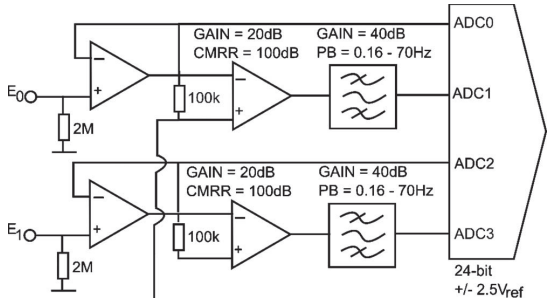

FIG. 3. Two channels of the eight-channel EEG amplifier. The nominal gain in the EEG channels (ADC1, ADC3, etc.) is 60 dB and the passband (PB) is 0.16 to 70 Hz. The input impedance is 2 MΩ. The unamplified channels (ADC0, ADC2, etc.) are used in the contact impedance measurement.

a 2 MΩ resistor network which connects the inputs of the measurement amplifier. Next, the signals are differentially amplified by 20 dB using an instrumentation amplifier (AD623, Analog Devices Inc., MA, USA) and the dc offset is removed using a 0.16 Hz lowpass feedback loop connected between the amplifier output and the reference pin. In the last stages, the signal is further amplified by 40 dB and filtered using a discrete 70 Hz Chebychev lowpass filter (single ended, four poles, 0.1 dB ripple). Digitalization is performed at 200 Hz using a 24 bit analog/digital (A/D) converter (LTC2449, Linear Technology Corporation, CA, USA) with a ±2.5 V reference.

The reference arrangement applied has been first introduced in the 1950s.[6] The idea is that the resistor network will force the isolated ground to float at a potential very close to the test subject's body. This keeps the common-mode voltage small making the setup tolerant of common-mode interference. On the other hand, the arrangement is also sensitive to variation in the electrode contact impedances because of the loaded input impedances and the voltage divider effect.[7,8] This may reduce the common-mode rejection ratio,[7] particularly when the number of electrodes is small. To avoid complications, the network resistance has to be fitted according to the number of channels and the electrode contacts have to be prepared carefully.[8] The present design tolerates a 20 kΩ contact impedance variation. This is sufficient because the contact impedance does not exceed 10 kΩ if the contacts are properly prepared.[9]

C. Audio stimulation system

Audio files are stored on a memory card (multimedia card) in wave-sound format and the playlist (i.e., the measurement paradigm) is saved in the memory of the MCU. The files are read and played using an application-specific audio decoder and amplifier chip (VS1011e, VLSI Solution, Finland) (Fig. 4). The MCU gives commands to seek, load, and play and takes care of the timing of the presentation of the stimuli.

The stimulation is conventionally performed by an external device. Thus, the arrangement applied simplifies the construction of the system and saves computer resources. In addition, it also allows accurate timing of the stimulus pre-

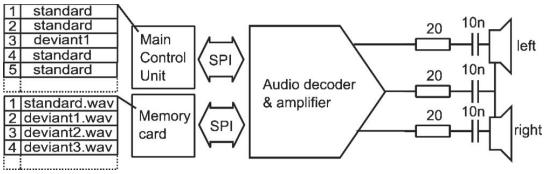

FIG. 4. Audio stimulation system. The order of the stimuli is stored in the memory of the main control unit, which controls the audio decoder that generates the audio signal. Audio files are saved on a memory card.

sentation because the process can be carried out as a first priority task in the embedded system. This is important because the jitter in the interstimulus interval (ISI) might otherwise cause the average responses to flatten, and produce changes in the physiological response studied.[4,9]

D. Other relevant functions

If a separate contact impedance meter is not available, the system has an option for contact testing which can be applied to verify the quality of the contacts while establishing the electrode connections. The impedances are estimated by feeding a test sine signal (300 mV, 23.2 Hz) to the cheek electrode and measuring the attenuation at other electrode sites. The raw test signal is generated by using 1 kHz pulse width modulation. The dc offset is corrected using a buffered 0.16 Hz highpass filter and the signal is smoothed by a passive 31 Hz lowpass resistor-capacitor (RC) filter. The test signal is fed to the test electrode through a 2 MΩ series resistor in order to avoid disturbing the referential balance.

E. Packing and layout

The layout (Fig. 5) is divided into a measurement board and a control board stacked inside the head box so that the form factor of the device is comfortable. The measurement board includes the EEG amplifier, A/D converter, and dc decoupling and feeding circuit for the contact impedance test. The control board includes the MCU, bluetooth module, and the audio generator. Module interconnection is through a 10 pin connector which includes a serial control bus [four-wire serial peripheral interface bus (SPI)], +8.4 V supply voltage (VCC), ground and contact test signal.

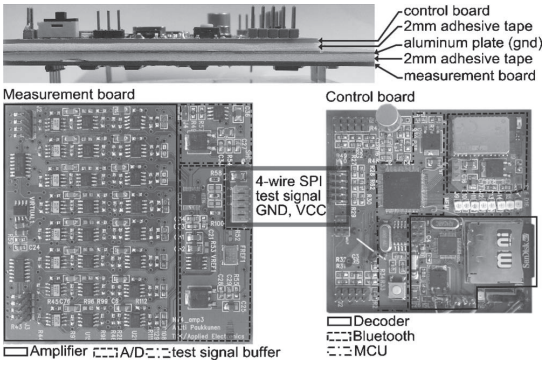

FIG. 5. Packing and layout of the electronics in the head box. The design is divided into two modules: a measurement board and a control board. These are stacked and a metal plate is placed in between them to prevent digital cross talk.

TABLE I. Technical performance of the prototype device. V_{ac} refers to alternating current voltage and V_{dc} refers to direct current voltage. Standard deviation is abbreviated as SD and ISI refers to the inter-stimulus interval (onset to onset).

No.	Test parameter	Measured value	Requirements
1	Power consumption (mW)	730–1100	<1470
2	Gain (dB)	60.6 ± 0.13	$< \pm 0.42$
3	Dynamic range ($V_{ac} \pm V_{dc}$) (mV)	2.3 ± 250	$>1 \pm 150$
4	Noise level at 0.16–70 Hz (μV_{rms})	0.64 ± 0.08	<0.5
5	Stimulus jitter (SD) (ms)	0.4 ± 0.1	<2.5

To reduce digital signal interference in the EEG path, a metal plate is placed in between the modules and the analog and digital circuits are physically separated so that they only meet at one single point near to the power supply. This arrangement forms a low-impedance path for the interference currents and reduces the amount of interference current coupling between the separated circuits. Each supply voltage is regulated separately.

III. TESTS AND RESULTS

A. Technical evaluation

The technical evaluation included measuring the power consumption, gain per channel, dynamic range, noise level, and ISI jitter produced by the audio stimulation system. The results are summarized in Table I.

A rechargeable, 8.4 V, 250 mA h, NiMH battery is used and thus the maximum allowable continuous power consumption is 1470 mW (70% of battery life and 1 h operation). The measured total power consumption was about 870–1100 mW in the active state and 730 mW in the resting state. The amplifier consumes about 15 mW, while the digital parts consume about 720–1080 mW, depending on the state of the audio stimulator device and the amount of data transmitted.

The nominal gain per channel is 60 dB (ac) and 20 dB (dc), giving an input range of 2.5 $mV_{ac} \pm 250$ mV_{dc}. This should allow an adequate signal range including artifacts[10] and the dc offset caused by the polarization of the electrodes.[11,12] The noise level defines the detection threshold for the target responses[2] and a generally acceptable target value is 0.5 μV_{rms} at the measurement band (0.16–70 Hz).[13,14]

The same limit (0.5 μV_{rms}) also applies to the gain and interchannel gain mismatch products. As the expected signal range is about 1–10 μV and the nominal gain is 60 dB, the gain mismatch should be less than ±0.42 dB [standard deviation (SD)]. The measured gain was 60.6 dB ± 0.13 dB (mean ± SD) and the noise base level was 0.72 ± 0.16 μV_{rms} (mean ± SD), which was reduced to 0.64 ± 0.08 μV_{rms} (mean ± SD) by digital filtering. One channel deviated from the others and showed 1.1 μV_{rms} noise but this was reduced to 0.7 μV_{rms} by digital filtering.

Jitter was measured by recording the stimulus stream with a PC microphone and analyzing the variation in the ISI

TABLE II. Description of the artifact detection method applied. V_x refers to the EEG signal recorded from electrode location x, μ represents the mean value, σ^2 represents the variance, and μ_{500} refers to 500 ms running average computed from the monitored signal.

No.	Artifact type	Formula	Window size (ms)	Detection threshold
1	Saccade	$V_{F8}-V_{F7}$	500	8 μV
2	Blink	$\mu(V_{Fp1},V_{Fp2})-\mu(V_{A1},V_{A2})$	75	8 μV
3	Face movement	$\mu(V_{Fp1},V_{Fp2})-\mu(V_{A1},V_{A2})$	500	$1.5-1.8\times\mu_{500}$
4	Bite	$\mu[\sigma^2(V_{A1}),\sigma^2(V_{A2})]$	500	$2-3\times\mu_{500}$

from the data acquired. The jitter does not affect the averaging process if it is less than half of the sampling period. Thus, while the sampling rate was 200 Hz, the maximum criterion for the jitter test is 2.5 ms. The measured interstimulus jitter was less than 1 ms (SD).

B. Demonstration

Three test subjects (healthy males, right handed, 24–29 years) were presented with auditory stimuli according to the classic Oddball paradigm ($p=0.2$, ISI=1014 ms) in a mismatch negativity[15] (MMN) study. The standard stimulus was a 75 ms, harmonic, sinusoidal tone with two harmonics (523, 1046, and 1569 Hz). The deviants differed either in frequency (+50 Hz), duration (−50 ms), or temporal structure (a 5 ms silent period in the middle of the stimulus). The evoked responses were recorded from Fp1, Fp2, F7, F8, Fz, and Cz according to the international 10–20 electrode system[16] and the signals were rereferenced to the mean of the mastoids (A1, A2). Electrode contacts were prepared so that the impedances would not exceed 5 kΩ.

Furthermore, the data processing interface was applied to preanalyze the recorded responses online. Artifact rejection was automated by allowing data dismissal when certain threshold values are exceeded. The detection threshold for the eye-related artifacts is constant while the base value for the other tests is determined on the basis of 500 ms running average of the signal being monitored (Table II). In addition, the conclusion of the experiment was also automated by applying our autoadaptive recording procedure.[17] The monitored parameters were the SNR and remaining measurement error (ERR) and the experiment was continued until the data quality met the predefined criteria (SNR > 0.69, ERR < 1.3 μV).

An example of the recorded responses and computed difference curves is presented in Fig. 6 and the test statistics are summarized in Table III. The amplitude of the AEPs that were recorded was 1.4–7.3 μV, depending on the stimulus type and the test subject. The estimated SNR of the averages varied from 2.7 to 104 (linear scale), and the remaining measurement error varied between 0.2 and 1.3 μV. 23%–51% of the data was discarded due to artifacts.

The MMN was analyzed from Fz and it was parametrized in a 20 ms average time window centered at the maximum of the difference of the average responses to the standard and deviant tones within 100–250 ms[18] from stimulus onset. Depending on the stimulus type and the test subject, the magnitude of the response was 1.5–4.5 μV and the latency varied from 125 to 175 ms. The statistical significance of the results was estimated by performing a paired t-test for the difference of the responses to the deviant stimuli and the response to the standard stimulus. All the responses were statistically significant ($p<0.05$), except the duration deviant with test subject 3 ($p=0.27$).

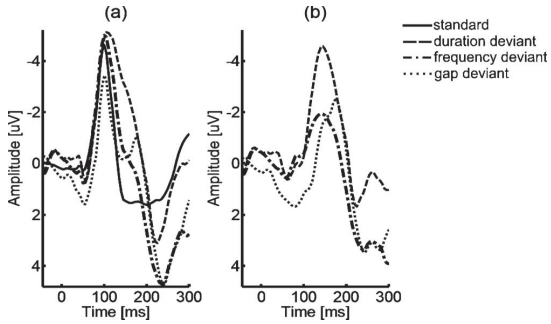

FIG. 6. An example of the responses recorded (test subject 2). (a) Average responses to the standard sound and the deviant sounds (duration, frequency, and gap). (b) Difference of the average response to the standard sound and the average response to each of the deviant sounds. The mismatch negativity appears as a peak in the difference curves at the latency of 140 to 175 ms, depending on the type of the deviant sound.

IV. DISCUSSION

The prototype presented here meets the predefined requirements and the expected operating time is about 1.5 h, good enough for 1 h measurements. Enhancements in the signal processing capability in the embedded system will further improve this figure through minimized communication channel needs. The dynamic range was also acceptable (2.3 $mV_{ac} \pm 250$ mV_{dc}), but the amplifier noise slightly exceeded specifications. This can be solved by component selection. The measured jitter in the stimulation system was less than 1 ms, which is adequate for AEP recordings.

TABLE III. Measurement statistics from the demonstration experiment. 1–3 refer to the average responses recorded, 4–6 refer to the computed MMN response, and 7–8 indicate to the quality of the data, in general.

No.	Test subject number	1	2	3
1	Amplitude of AEPs (μV)	5.3–7.3	3.4–5.1	1.4–4
2	Signal-to-noise ratio of AEPs	8.6–104	2.7–41	4–54
3	Remaining measurement error (μV)	0.2–1.3	0.3–1.3	0.4–1.2
4	Amplitude of MMN responses (μV)	2.8–3.3	1.9–4.5	1.5–2.9
5	Latency of MMN responses (ms)	155–175	140–175	125–145
6	*P* value of MMN responses (t-test)	<0.01	<0.01	0.0005–0.27
7	Accepted standard responses (pcs)	1011	892	1123
8	Accepted deviant responses (pcs/type)	76–81	66–70	80–89
9	Trial rejection ratio (%)	23	51	47

Average responses were successfully recorded from all three test subjects and a statistically significant MMN ($p < 0.05$) was found in eight out of nine test cases. A differential response was present also in the missing case (duration deviant, test subject 3), but was not statistically significant ($p = 0.27$). This was probably caused by a small artifact peak that had passed the rejection process as a result of the inevitable compromises between the protection of valid data and the amount of artifact feedthrough. Lowering the artifact detection thresholds without an increase in the loss of data requires improvements in the artifact rejection tools.

ACKNOWLEDGMENTS

We wish to thank P. Eskelinen, H. Rimminen, and our other colleagues for valuable discussions. We also want to thank H. Ruotoistenmäki and K. Rajala for their contribution to the mechanical design. The work was supported in part by the Graduate School of Electrical and Communications Engineering and Society of Electronics Engineers.

[1] C. C. Duncan, R. J. Barry, J. F. Connolly, C. Fischer, P. T. Michie, R. Näätänen, J. Polich, I. Reinvang, and C. van Petten, Clin. Neurophysiol. **120**, 1883 (2009).
[2] A. H. Lang, O. Eerola, P. Korpilahti, I. Holopainen, S. Salo, and O. Aaltonen, Ear Hear. **16**, 118 (1995).
[3] A. C. Metting van Rijn, A. A. Peper, and C. A. Grimbergen, Med. Biol. Eng. Comput. **28**, 389 (1990).
[4] E. Pekkonen, T. Rinne, and R. Näätänen, Electroencephalogr. Clin. Neurophysiol. **96**, 546 (1995).
[5] J. Sinkkonen and M. Tervaniemi, Audiol. Neuro-Otol. **5**, 235 (2000).
[6] F. F. Offner, Electroencephalogr. Clin. Neurophysiol. **2**, 213 (1950).
[7] J. W. Osselton, Electroencephalogr. Clin. Neurophysiol. **19**, 527 (1965).
[8] A. Paukkunen and R. Sepponen, Med. Biol. Eng. Comput. **46**, 933 (2008).
[9] T. W. Picton, S. Bentin, P. Berg, E. Donchin, S. A. Hillyard, R. Johnson, Jr., G. A. Miller, W. Ritter, D. S. Ruchkin, M. D. Rugg, and M. J. Taylor, Psychophysiology **37**, 127 (2000).
[10] L. Sörnmo and P. Laguna, *Bioelectrical Signal Processing in Cardiac and Neurological Applications* (Elsevier, Burlington, MA, 2005).
[11] L. A. Geddes, *Electrodes and the Measurement of Bioelectric Events* (Wiley, New York, 1972).
[12] P. Tallgren, S. Vanhatalo, K. Kaila, and J. Voipio, Clin. Neurophysiol. **116**, 799 (2005).
[13] P. Tiihonen, J. Kinnunen, J. Töyräs, E. Mervaala, and A. Pääkkönen, Comput. Methods Programs Biomed. **89**, 83 (2008).
[14] M. R. Nuwer, G. Comi, R. Emerson, A. Fuglsang-Frederiksen, J.-M. Guérit, H. Hinrichs, A. Ikeda, F. J. C. Luccas, and P. Rappelsburger, Electroencephalogr. Clin. Neurophysiol. **106**, 259 (1998).
[15] R. Näätänen, A. W. K. Gaillard, and S. Mäntysalo, Acta Psychol. **42**, 313 (1978).
[16] F. Sharbrough, G-E. Chatrain, R. P. Lesser, H. Lüders, M. Nuwer, T. W. Picton, J. Clin. Neurophysiol. **8**, 200 (1991).
[17] A. K. O. Paukkunen, M. Leminen, and R. Sepponen, Front. Neuroeng. **3**, 2 (2010).
[18] E. Schröger, Behav. Res. Methods Instrum. Comput. **30**, 131 (1998).